Spatial-coherence modulation for optical interconnections

Betty Lise Anderson and Lawrence J. Pelz

The spatial coherence of a laser beam depends on the number and the relative weights of the spatial modes supported by the laser waveguide. By electro-optic modulation of the cavity geometry, the spatial-coherence function can be modulated between zero and one at predictable locations across the beam and thus carry information. A simple integrated-optic interferometer is used to decode the signal. Spatial coherence can be modulated independently of the beam intensity and can be used as another level of multiplexing in addition to amplitude modulation, wavelength-division modulation, etc. One can implement a free-space optical interconnection scheme by carrying data on the intensity and address information on the spatial coherence. © 1995 Optical Society of America

1. Introduction

Free-space optical interconnections promise high-speed data transfer in a variety of applications, including internal communications within mainframe computers and board-to-board or interchip data transfer. A significant problem is that of how to carry the data and the address on the same signal and allow for changing addresses, all at high speed with little cross talk. For example, carrying the data and the address on different polarizations has been proposed.[1,2] Reconfigurable holograms have also been discussed to allow changing addresses in a system.[3,4] Another area for development in free-space communications is that of increasing capacity of existing optical data links, for example, by addition of increased levels of multiplexing.

Coherence multiplexing can add this dimension. Temporal-coherence multiplexing (sometimes called path-difference multiplexing) has been demonstrated.[5–8] It exploits the finite temporal coherence of a source and uses various delays to remove the coherence between signals. The signals are then decoded by multiple power splitters and another set of delay lines.

Here, however, rather than temporal coherence, we discuss using spatial-coherence multiplexing, which is based on entirely different principles. Whereas temporal or longitudinal coherence compares the correlation of a beam with a time-delayed version of itself, spatial coherence measures the correlation between two points on the same wave front, i.e., at the same point in time, thus eliminating the optical delay lines. In a nutshell, the principle used here is based on the fact that the spatial-coherence function (SCF) of a source is directly determined by the number and the weights of the spatial modes supported by that source. By modulating the amount of energy in these spatial modes, one can make the spatial coherence vary between zero and one, providing (ideally) a perfect extinction ratio.

2. Theory

We begin by briefly reviewing the definition of spatial coherence, the correlation between two points (x_1, x_2) on a particular wave front (as opposed to temporal coherence, which measures correlation between two different wave fronts). The relationship between the cross-spectral density $W(x_1, x_2, \omega)$ and a set of natural modes of a system has been explored in the space frequency domain.[9–11] We choose, however, to describe the system in the time domain, in terms of its spatial coherence $\gamma(x_1, x_2, \tau)$ and its spatial modes, where τ is a time delay. The classical way to measure spatial coherence is to use Young's double slits (Fig. 1), which we use for a moment to illustrate the physics. The slits sample the beam at two points, and a fringe pattern is produced on the observation screen because of the path difference δ. This path difference between the two diffracted beams is assumed to be much less than the temporal-coherence

The authors are with the Department of Electrical Engineering, The Ohio State University, 205 Dreese Laboratory, 2015 Neil Avenue, Columbus, Ohio 43210.

Received 23 December 1994; revised manuscript received 12 June 1995.

0003-6935/95/327443-08$06.00/0.

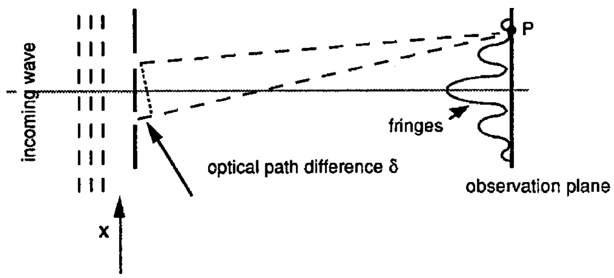

Fig. 1. Young's double-slit geometry for measuring spatial coherence.

length. The visibility of the fringes is a measure of the spatial coherence.

If we call the field arriving at point P from slit 1 $E(x_1, t_1)$, and if the field arriving from slit 2 is $E(x_2, t_2)$, where t is arrival time, then the total field arriving at P is $E(x_1, t_1) + E(x_2, t_2)$. A detector at point P would measure the intensity

$$I(P) = \langle [E(x_1, t_1) + E(x_2, t_2)]^* [E(x_1, t_1) + E(x_2, t_2)] \rangle, \quad (1)$$

where

$$E(x_1, t_1) = A(x_1)\exp(-i\omega t)\exp(-i\omega t_1),$$
$$E(x_2, t_2) = A(x_2)\exp(-i\omega t)\exp(-i\omega t_2). \quad (2)$$

Combining Eqs. (1) and (2), we obtain [letting $A_1 = A(x_1)$]

$$I(P) = \langle A_1^2 + A_2^2 + 2A_1A_2 \cos \omega\tau \rangle$$
$$= I_1 + I_2 + 2(I_1I_2)^{1/2}\mathrm{Re}[\gamma_{12}(\tau)], \quad (3)$$

where $\tau = t_1 - t_2 = kn\delta$ is the relative time delay between the two beams, I_1 is the intensity at the slit located at x_1, I_2 is the intensity at the slit located at x_2, n is the refractive index, and $\gamma(\tau)$ is the normalized mutual-coherence function

$$\gamma_{12}(\tau) = \frac{\langle E^*(x_1, t)E(x_2, t + \tau)\rangle}{(I_1I_2)^{1/2}}. \quad (4)$$

The quantity $\gamma_{12}(\tau)$ measures the correlation between the fields at the two slits, or two specific spatial points on the wave front. The visibility of the interference fringes V is defined as

$$V = \frac{I_{\max} - I_{\min}}{I_{\max} + I_{\min}}, \quad (5)$$

where $I_{\max}$ is the peak intensity of the fringes and $I_{\min}$ is the lowest intensity. It can then be shown that[12]

$$V = \frac{2(I_1I_2)^{1/2}}{I_1 + I_2}|\gamma_{12}(\tau)|, \quad (6)$$

or, if $I_1 = I_2$, the fraction in Eq. (6) goes to 1, and the visibility is directly equal to the spatial coherence $\gamma_{12}(\tau)$.

It turns out that the spatial coherence relates directly to the spatial mode structure of a beam. Consider a waveguide that supports some set of n orthonormal modes $f_n(x)$, where x is one of the two directions across the wave front, perpendicular to the direction of propagation z. If each mode has a particular weight a_n, the total field distribution across the waveguide can be written as (neglecting the y dependence)

$$E(x, z, t) = \sum_n a_n f_n(x)\exp[i\varphi_n(x, z, t)]. \quad (7)$$

For example, a waveguide supporting Hermite–Gaussian modes has, as its f_n values,

$$f_n(x) = \left[\frac{2}{\pi w^2(z)}\right]^{1/4}\left[\frac{1}{(2^n n!)^{1/2}}\right]H_n\left(\frac{\sqrt{2}x}{w(z)}\right)\exp\frac{-x^2}{[w^2(z)]}, \quad (8)$$

where the factors in front are normalizing coefficients, H_n is the Hermite polynomial of order n, and $w(z)$ is the beam's spot size. If $n = 0$, then $H_n(\alpha) = 1$, and the lowest-order mode has a pure Gaussian distribution.

The interference pattern resulting from two symmetrically chosen points x and $-x$ on the beam is given by

$$I(x, -x, \tau) = \langle [E(x, t) + E(-x, t + \tau)]^* \times [E(x, t) + E(-x, t + \tau)]\rangle, \quad (9)$$
$$= \sum_n a_n^2 f_n^2 + \sum_n a_n^2 f_n^2(-x) + 2\,\mathrm{Re}\left[\sum_n a_n^2 f_n(x) f_n(-x)\exp(-i\omega\tau)\right]. \quad (10)$$

The third term in Eq. (10) is the (unnormalized) mutual coherence. If we arrange our experiment such that the time difference τ is zero, for example, by placing point P in Fig. 1 on the optical axis, then[13]

$$\gamma(x, -x, 0) = \left|\sum_n a_n^2 f_n(x) f_n(-x)\right| \times \left[\sum_n a_n^2 f_n^2(x) \sum_n a_n^2 f_n^2(-x)\right]^{-1/2}, \quad (11)$$

which varies with the measurement points $(x, -x)$, i.e., the spacing of the slits. This can be rewritten as

$$\gamma(x, -x, 0) = \left[\frac{I_{\max}(x) - I_{\min}(x)}{I_{\max}(x) + I_{\min}(x)}\right]\frac{I(x) + I(-x)}{2[I(x)I(-x)]^{1/2}}, \quad (12)$$

where $I(x) = \sum_n a_n^2 f_n^2(x)$, $I(-x) = \sum_n a_n^2 f_n^2(-x)$, and $I_{\max}(x)$ and $I_{\min}(x)$ are the maximum and the minimum intensities obtained on the interference pattern.

When functions describing the transverse-mode structure satisfy the symmetry condition $f_n^2(x) = f_n^2(-x)$ (as do Hermite–Gaussian modes), Eq. (12)

takes the simple form

$$|\gamma(x, -x, 0)| = \frac{I_{\max}(x) - I_{\min}(x)}{I_{\max}(x) + I_{\min}(x)} = V. \tag{13}$$

For a beam containing only one spatial mode, the spatial coherence γ is unity everywhere. When a second mode is present, however, the SCF has well-defined zeros, whose positions can be shown to be at[14]

$$x = \pm \frac{w(z)}{2} \frac{a_0}{a_1}, \tag{14}$$

where, again, a_0 and a_1 are the relative field strengths of modes 0 and 1, and $w(z)$ is the beam spot size at some location z [Eq. (8)]. For example, Fig. 2(a) shows the field distributions for the zeroth and the first modes individually. Figure 2(b) shows the intensity distribution for a source that has (i) only the fundamental mode and (ii) both modes, with the zeroth mode supplying 90% of the energy and the first mode 10%. Note that these two intensity distributions are virtually indistinguishable and that the total intensities are identical. Figure 2(c) shows that a dramatic change occurs in the SCF, however. When only one mode is present, the fringe visibility is perfect (unity) for any two symmetrically chosen points (i.e., any slit spacing). When the second mode is present, even in very small amounts, the SCF and thus the fringe visibility go to zero for certain positions on the beam (a particular slit spacing). One can control the positions of these zeros by controlling the relative energy in the higher-order mode, according to Eq. (14).

Some care must be taken in choosing where the zeros fall. The lower the relative weight of the higher-order mode, the farther from beam center the zeros occur. These can occur so far from beam center so as to be not directly measurable because the intensity drops off to an infinitesimally small value. Figure 3 shows the SCF's for varying values of a_0^2/a_1^2

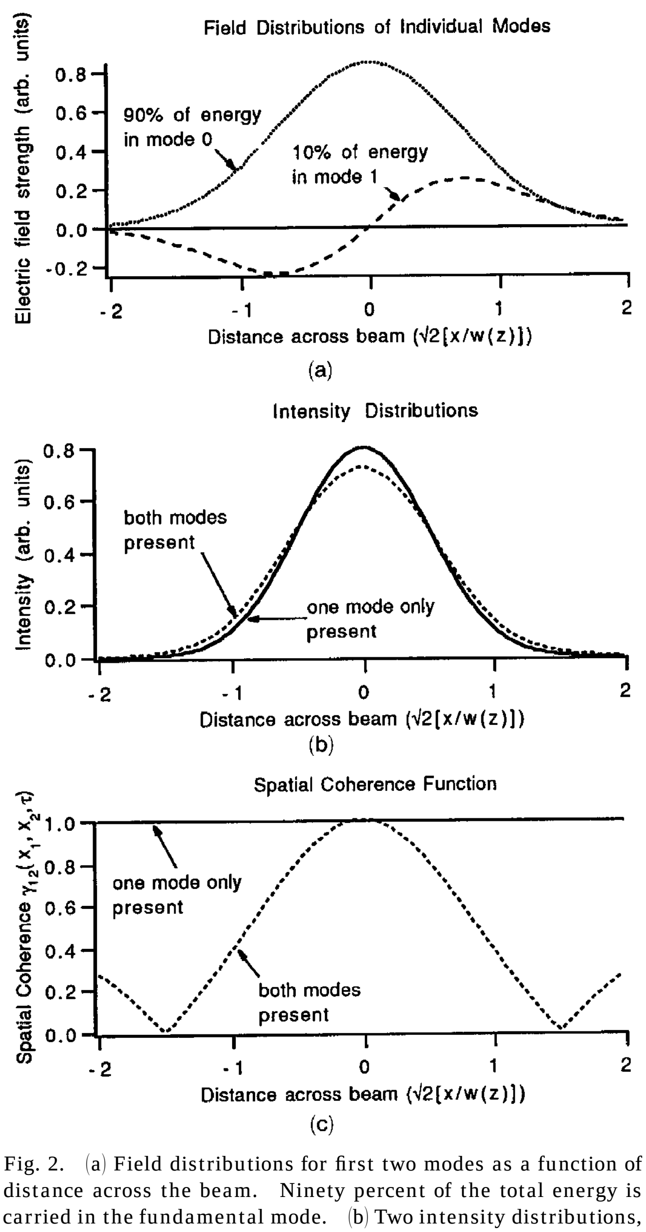

Fig. 2. (a) Field distributions for first two modes as a function of distance across the beam. Ninety percent of the total energy is carried in the fundamental mode. (b) Two intensity distributions, one with all energy carried in the zeroth mode, the other with a 90:10 energy distribution as in the first graph. (c) SCF's for the same two cases.

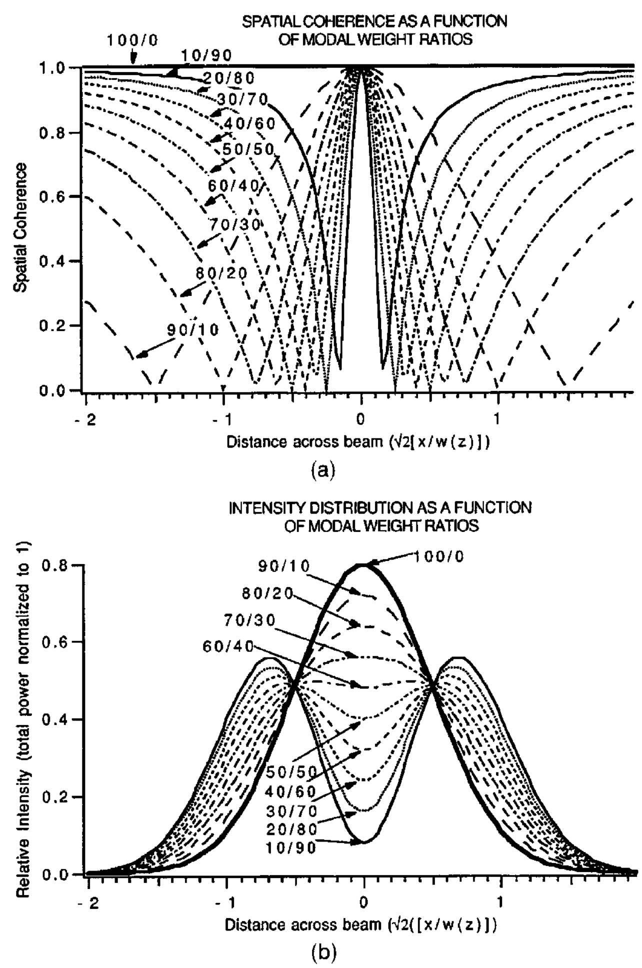

Fig. 3. (a) SCF's and (b) intensity distributions for various percentages of the total energy in fundamental/first modes.

(we are expressing energy ratios rather than field-strength ratios) along with the corresponding intensity profiles. For example, to have the zeros appear at a point on the beam where the intensity is still at least $1/e$ of the fundamental mode's intensity distribution, a_0^2/a_1^2 should be at least 0.65/0.35. The drawback is that for this ratio of a_0^2/a_1^2, the intensity at $\pm x$, where x is the location of the SCF zero, varies by 27% between the single-mode and the two-mode cases. The only case for which the intensity remains unchanged at these two points $\pm x$ (as opposed to the total intensity, which does remain constant) is the case in which each of the two modes carries 50% of the total energy. In the modulator discussed below, however, the waveguide geometry, and therefore the intensity distribution, changes slightly between the single-mode and the dual-mode cases, so the 50/50 ratio also needs to be adjusted slightly.

A laser that emits the zeroth and the first modes in these weights may, however, also support additional higher-order modes. When these additional modes are present, the spatial coherence does not necessarily go to zero, but rather can have maxima and minima, or multiple zeros. Several examples of SCF's are shown in Fig. 4, in which three or more modes are allowed, again assuming Hermite–Gaussian modes. The locations of the minima, the maxima, and the zeros can be found by determination of the inflection points of Eq. (11).

Some discussion of these cases is necessary. For example, for reasonable values of a_0, a_1, and a_2, maxima and minima appear in the SCF. A pair of interferometers looking at $\pm x_1$ and $\pm x_2$, respectively, might each look for the coherence to be within a certain range, producing a 2-bit code that identifies the particular mode structure.

Another possibility is to vary a structure from supporting a single spatial mode to one supporting three modes, of weights such as those in Fig. 4(b). Then the SCF is close to zero over a somewhat wider range of $\pm x$ values than for a case with only one pronounced SCF zero, possibly easing design constraints at the receiver. This possibility is also attractive because of relatively high intensity at the $\pm x$ locations of the zeros.

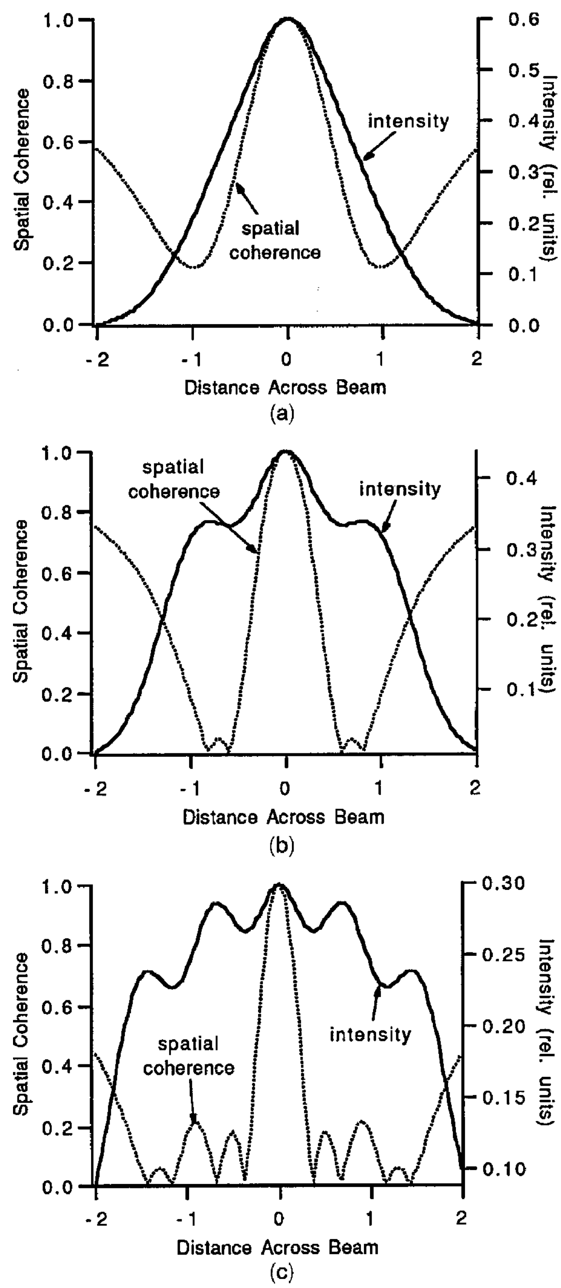

Fig. 4. Examples of arbitrary cases in which more than just the first two modes are present: (a) The first three modes are present in the energy ratio of 70:20:20 (zeroth:first:second); (b) the relative strengths of the first three modes are 40:30:30; (c) the first five modes present in equal weights.

3. Modulation of the Spatial Coherence

We have shown that the spatial-coherence function depends directly on the spatial modes. The number of spatial modes supported by a laser or some other waveguide depends on the refractive-index profile and the waveguide dimensions. Therefore one can modulate the existence and the strength of specific spatial modes by modulating either the cavity refractive-index profile or the cavity dimensions, or both. Because it is difficult in practice to vary the refractive-index profile of a laser cavity electrically without affecting the gain and therefore the intensity, we consider the case of an external modulator of a structure similar to that in Fig. 5(a). The center waveguide is passive and supports a single lateral mode. (We use the convention of the semiconductor field, in which lateral refers to the direction parallel to the junction plane or surface, and transverse the direction perpendicular to the surface. These can, in principle, be modulated independently, but we consider only lateral-mode modulation here.) There are, in addition, electro-optically controllable outrigger waveguides, whose index can be varied to match either that of the substrate, in which case the device supports only the fundamental mode, or that of the center waveguide, effectively widening it enough to

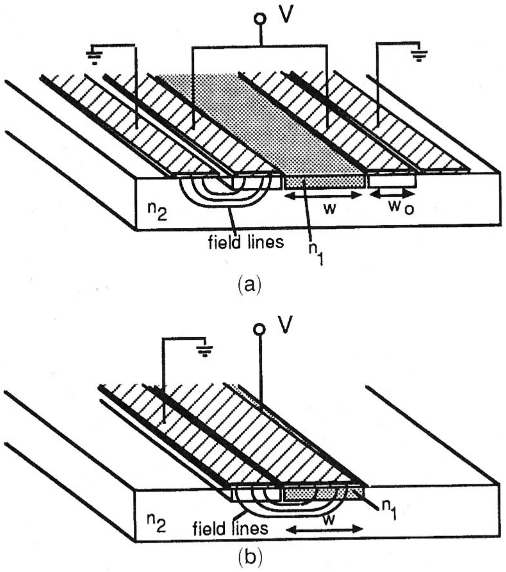

Fig. 5. Two proposed external modulator structures: (a) center passive core, with electro-optically controlled outrigger waveguides; (b) single core, where waveguide Δ is electro-optically controlled.

support the first higher-order mode. By varying the control voltage, one alternately cuts off or allows this second mode to propagate, which in turn causes the SCF to vary from unity everywhere to some function such as those in Fig. 3. Electro-optic modulators that intensity modulate a signal by electro-optically varying the refractive index to cut off or to allow the fundamental mode have already been demonstrated.[15]

An alternative SCF modulator structure is shown in Fig. 5(b) and contains a single waveguide core, whose refractive index is electro-optically controlled. In this geometry, the refractive-index difference ($\Delta = 1 - n_{\mathrm{cladding}}/n_{\mathrm{core}}$) is varied, resulting in a change in the number of allowed modes.

The amount of energy in each mode depends not only on the waveguide itself but also on how the input beam is coupled to the waveguide, as well as any opportunities for mode coupling as the beam travels the waveguide. However, these remain constant in a particular system, and the input coupling can be adjusted to fine tune the SCF zero locations.

Electro-optic materials such as lithium niobate may be used, but to integrate the source and the modulator on one semiconductor chip, one can implement the modulator section in reverse-biased multiple quantum wells, which are known to have strong electro-optic effects.[16,17]

These perfectly symmetric rectangular geometries exhibit close approximations to Hermite–Gaussian modes. It must be realized, however, that the shape of the fundamental mode (its width) changes when the waveguide is changed. Figure 4 was generated assuming the fundamental mode remains the same, and higher-order modes are added *to the same waveguide.* To accurately determine the change in local intensities at $\pm x$, one must take into account the change in mode shape from one case to the other.

For example, consider the case of a symmetric dielectric slab waveguide, of the configuration shown in Fig. 5(b). Assume that the waveguide is x-cut $LiNbO_3$, whose r_{33} is 30.9×10^{-12} m/V.[18] The index of the waveguide core is 2.208 (no voltage applied), that of the substrate is 2.2075 ($\Delta = 0.0005$), and its width is 5 µm. Then at a wavelength of 633 nm the first higher-order mode is cut off. When the waveguide's index is changed electro-optically to a Δ of 0.001, two modes are allowed. The voltage necessary to do this depends on the placement of the electrodes and the depth of the waveguide but is of the order of 20 V or less. Figure 6 shows the calculated field distributions for the supported modes for each case.[19] Note that there is a difference between the two energy distributions, and there is a difference between the fields of the fundamental modes as well. Also shown are the spatial-coherence functions for each case, assuming a 50/50 energy distribution between the fundamental and the first modes for the two-mode case. At the point at which the SCF zeros appear (dashed curves), the intensity change is negligible between the two cases.

4. Detection

To detect the mutual coherence between the points $\pm x$ on the beam, one needs an interferometer that

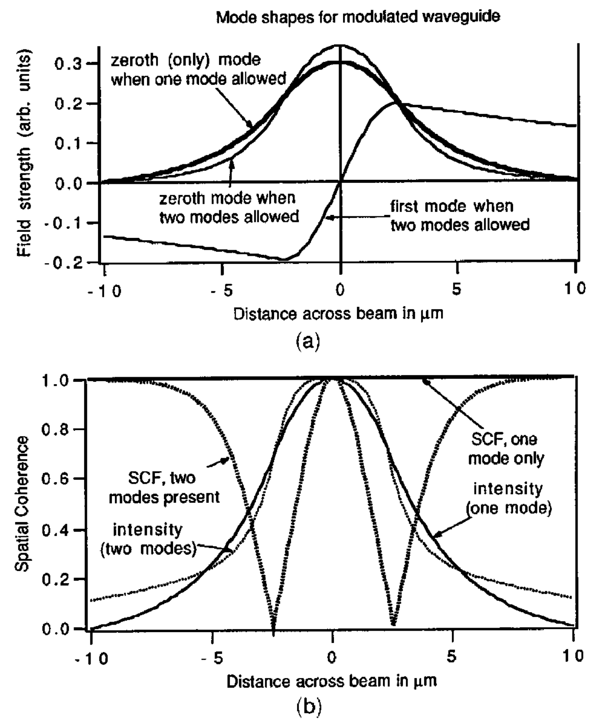

Fig. 6. Mode shape of the fundamental mode changes slightly when the waveguide geometry is electro-optically altered: (a) The thick curve is the mode-field distribution when only one mode is allowed. The thin curves are the fields of two allowed modes (equal weights). (b) SCF's and overall intensity for the single-mode and the dual-mode cases. Despite modes not being exactly Hermite–Gaussian and that mode shapes change slightly between the two cases, a 50/50 ratio of mode energies for the two-mode case still gives a negligible intensity change at the interferometer arms ($\pm x$ located at the dashed curves).

samples the beams at those two points. Slits are not practical because of alignment problems, because they rely on diffraction, which spreads the small energy from each samples across the entire observation plane necessitating high-energy signals, and because it would be difficult to measure the fringe visibility at high speeds.

A technique for measuring spatial coherence with a twin-fiber interferometer has been demonstrated,[20] in which two arms of a directional fiber coupler are placed at the sample points $\pm x$. The fields at $\pm x$ are summed in the coupler. One fiber is physically translated a short distance, much shorter than the temporal-coherence length of the source, introducing a varying phase delay. This causes fringes to appear if the fields at $\pm x$ are mutually coherent.

Here, however, one avoids the slowness of the mechanical motion by substituting a rigid, integrated optic directional coupler (Fig. 7), whose arms are fixed at the spacing $\pm x$ of the expected zeros in the SCF. The fields are summed in the coupler, and one introduces the phase difference by electro-optically varying the optical path length through one arm. The visibility of the resulting fringes yields the magnitude of SCF for $(x, -x)$. If a voltage ramp with a high slope is applied to the receiver's electro-optic arm, the refractive index can vary rapidly, resulting in fringes whose temporal frequency is faster than that of the other signals in the system, for example, the data. Therefore several fringes per clock cycle might be achieved. To determine the state of the spatial coherence, one needs to look for the presence or the absence of energy at this very high frequency. For example, the fastest photodetectors available at the time of this writing have a speed of 60 GHz.[21] Assuming several fringes are wanted per data bit, a signal rate of 20 GHz is reasonable and achievable with today's lithium niobate devices as well as semiconductor multiple-quantum-well modulators.

Let us consider several ways to exploit the modulation of the spatial coherence. In the simplest case, let us suppose that only the intensity (and not the SCF) is being modulated but that the detector is one such as that in Fig. 7 rather than a conventional intensity detector. The source is made, in this case, to support only the fundamental spatial mode, so that the SCF of the signal is unity regardless of the chosen spacing of the detector arms. The ambient light, assumed to be incoherent (room lights, sunlight, etc.), has the effect of adding a dc component to the fringes, which can be removed electrically with a high-pass filter. The amplitudes of the fringes themselves carry the information. The signals for such a case are shown in Fig. 8. Note that it is probably not practical to use spatial-coherence modulation for ambient-light filtering, as there are easier ways to do this, for example, with a high-frequency carrier. We give some numbers here, however, to show the relative optical powers: for a reasonable power level emanating from the modulator (1 mW), a reasonable beam size (collimated elliptical Gaussian with intensity spot sizes of 0.25 and 0.35 mm in the two orthogonal directions), and practical detector arm sizes (0.3 µm square), the power density at the receiver arms is ~20% that of the ambient light in bright sunlight. A high-pass filter should easily be able to separate the coherent and the incoherent components.

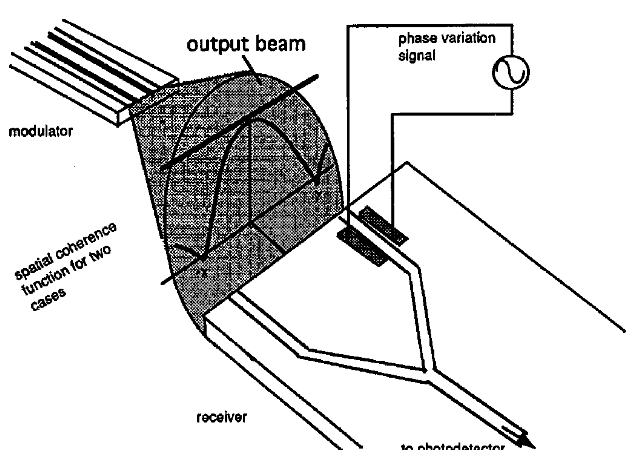

Fig. 7. The receiver distinguishes between zero coherence (two modes present) and perfect coherence (one mode present).

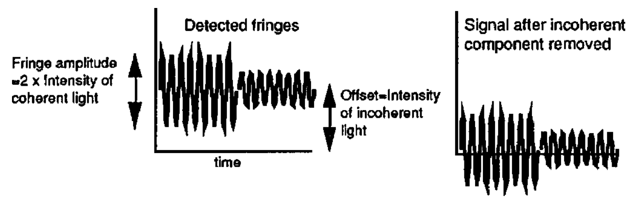

Fig. 8. Intensity is modulated, but spatial coherence is detected. Ambient (incoherent) light adds a uniform dc offset to the fringes.

Another possibility is to modulate the spatial coherence without modulating the intensity. In this case the detected signal would appear as in Fig. 9. When the modulator supports only the fundamental spatial mode, the coherence between the two interferometer arms is perfect, and fringes of unity visibility result (the first bit in Fig. 9) as the phase in the interferometer is varied. When the modulator is altered electrically to support the second mode, the SCF goes to zero at the prescribed locations x and $-x$, determined by the weights of the modes. In this case, for the proper choice of interferometer arm placement $\pm x$,

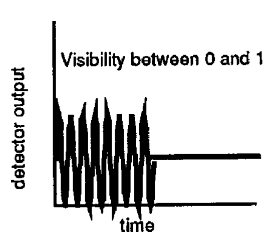

Fig. 9. Spatial coherence (but not intensity) is modulated; spatial coherence is detected. Energy found at the fringe frequency gives a one or a zero.

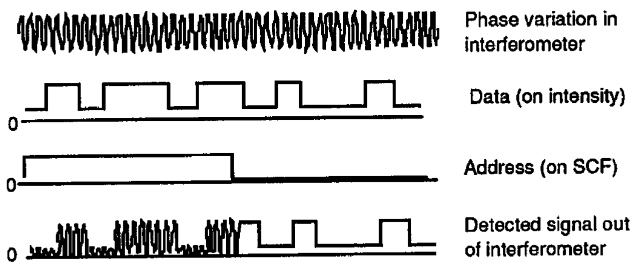

Fig. 10. Example of signals in a multiplexed system, in which data are carried by intensity modulation and the address is carried on the same beam on the spatial-coherence modulation.

the coherence is zero, which results in no fringes, just a constant intensity (second bit in the figure).

This application leads one to the idea of multiplexing the data and the address onto the same beam by using intensity to carry data and the spatial coherence to carry address information (Fig. 10). In this application, one might split the beam onto two detectors, one conventional intensity detector to retrieve the data and the other of the type in Fig. 7 to gather the address. Note that this also can be done electrically after the photodetector. For recovery of the address information, only the presence of fringes needs to be detected, not their amplitude, at least in the binary system as proposed here. (One could vary the spatial coherence continuously between 0 and 1, assigning various intervals to separate addresses, in which case the magnitude of the fringes compared with their average value must be computed. One could also, as mentioned earlier, have two interferometers, looking at $\pm x_1$ and $\pm x_2$, and the combination of these two values could carry the address information.)

In the SCF multiplexing scheme, a given detector, with a given arm spacing, is in effect asking, "Is this data signal intended for me?" by looking for a signal with no fringes. To allow for a variety of possible addresses, one can stack an array of interferometers,

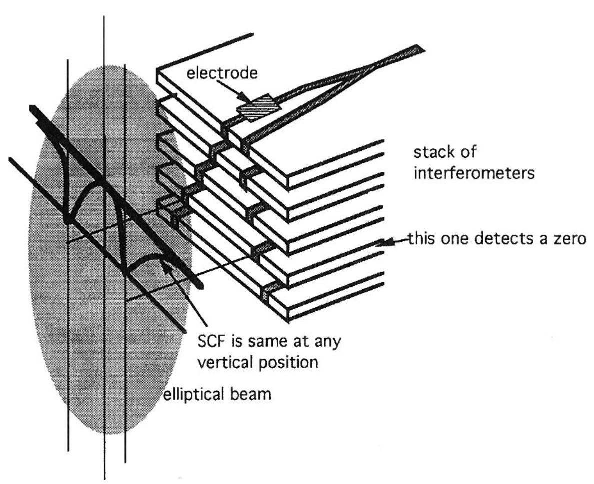

Fig. 11. Stack of interferometers. Data in this case are intended for the receiver that is second from the bottom. Others can detect but are programmed to ignore the data.

each with different arm spacing, as in Fig. 11. Each detector looks for zero coherence (no fringes) at its particular $\pm x$. Despite the fact that the beam's intensity falls off away from beam center, the spatial coherence between $\pm x$ is independent of the value of y on a wave front traveling in the z direction. A beam can be expanded in the y direction, for example, with a cylindrical lens, without affecting the spatial-mode structure in the x direction.

5. Discussion and Summary

There are three additional points to be made about use of the SCF to carry information. One is that the technique can be used only for free-space interconnections because coupling the light into any other waveguide, such as a fiber, imprints this waveguide's spatial modes onto the signal, obliterating the information. The second is that this system is not practical for long-distance applications, such as intersatellite communications. The reason that spatial-coherence modulation cannot be used is that the locations of the zeros are a function of relative position across the beam; as the beam expands, the zeros also move farther apart, making the construction of an interferometer with correctly spaced arms impractical for very long haul systems. If the interferometer is to be monolithic (i.e., arm spacing is not greater than 1 cm), the upper limit on the distance between the source and the receiver is of the order of a kilometer, assuming a wavelength of 633 nm. This is based only on beam spreading; atmospheric perturbations would reduce this distance considerably. The final point is that the coupling efficiency is low because the interferometer arms sample only a small quantity of the optical energy. In short-haul interconnections or communication links for which this technique is applicable, this would be less of a problem than it might otherwise be because there are no lengths of attenuating fiber, for example. The source power can be high but in fact need not be unusually high. We routinely measure the spatial coherence of laser beams having overall powers of the order of a few milliwatts using single-mode fiber (core diameter 5 μm) when the total energy per interferometer arm is as little as 2 pW.

Despite the points made above, the method described here of exploiting the spatial coherence as a carrier of information is still potentially useful. The SCF can be modulated instead of intensity to communicate data, or both intensity and spatial coherence can be modulated independently for added depth of multiplexing. These can be used in addition to other conventional types of multiplexing, such as frequency-division multiplexing and wavelength-division multiplexing. By imprinting the data on a beam's intensity and the intended receiver address on the SCF, one can broadcast a signal from a given source to a number of detectors, only one of which recognizes the data as intended for it. This results in a high-speed all-optical interconnection in which the address and the data can both be changed electronically with no mechanical movement or bulk optics.

This work was supported in part by National Science Foundation grant ECS-9108425.

References and Notes

1. R. B. Jenkins and B. D. Clymer, "Acousto-optic comparison switch for optical switching networks with analog addressing techniques," Appl. Opt. **31,** 5453–5463 (1992).
2. D. C. Butzer, B. L. Anderson, and B. D. Clymer, "Highly efficient interconnection for use with a multistage optical switching network with orthogonally polarized data and address information," Appl. Opt. **34,** 1788–1800 (1995).
3. J. W. Goodman, F. J. Leonberger, S.-Y. Kung, and R. A. Athale, "Optical interconnections for VLSI systems," Proc. IEEE **72,** 850–866 (1984).
4. B. L. Anderson, T. B. D. Vore, and B. D. Clymer, "Use of laser-diode arrays in holographic interconnections," Appl. Opt. **31,** 7411–7416 (1992).
5. K. W. Chu and F. M. Dickey, "Optical coherence multiplexing for interprocessor communications," Opt. Eng. **30,** 337–344 (1991).
6. H. Porte, J. P. Geodgebuer, and A. Hamel, "Two TV channel multimode fibre link using a single multilongitudinal mode laser diode (820 nm) and path-difference miltiplexing," Electron. Lett. **22,** 1189–1191 (1986).
7. J.-P. Goedgebuer and A. Hamel, "Coherence multiplexing using a parallel array of electrooptic modulators and multimode semiconductor lasers," IEEE J. Quantum Electron. **QE-23,** 2224–2236 (1987).
8. J. L. Brooks, R. H. Wentworth, R. C. Youngquist, M. Tur, B. Y. Kim, and H. J. Shaw, "Coherence multiplexing of fiber-optic interferometric sensors," J. Lightwave Technol. **LT-3,** 1062–1071 (1985).
9. A. Starikov and E. Wolf, "Coherent-mode representation of Gaussian Schell-model sources and their radiation fields," J. Opt. Soc. Am. **72,** 923–928 (1982).
10. E. Wolf, "New theory of partial coherence in the space–frequency domain. Part I: Spectra and cross spectra of steady-state sources," J. Opt. Soc. Am. **72,** 343–351 (1982).
11. E. Wolf, "New theory of partial coherence in the space–frequency domain. Part II: Steady-state fields and higher-order correlations," J. Opt. Soc. Am. A **3,** 76–84 (1986).
12. M. Born and E. Wolf, *Principles of Optics,* 6th ed. (Pergamon, New York, 1980).
13. P. Spano, "Connection between spatial coherence and modal structure in optical fibers and semiconductor lasers," Opt. Commun. **33,** 265–270 (1980).
14. L. J. Pelz and B. L. Anderson, "Practical use of the spatial coherence function for determining laser transverse mode structure," Opt. Eng. (to be published).
15. E. J. Patej, "Electro-optical mode extinction modulator in $LiNbO_3$," Opt. Eng. **33,** 1717–1719 (1994).
16. J. E. Zucker, I. Bar-Joseph, B. I. Miller, U. Koren, and D. S. Chemla, "Quaternary quantum wells for electro-optic intensity and phase modulation at 1.3 and 1.55 µm," Appl. Phys. Lett. **54,** 10–12 (1988).
17. T. H. Wood, R. W. Tkach, and A. R. Chraplyvy, "Observation of large quadratic electro-optic effect in GaAs/AlGaAs multiple quantum wells," Appl. Phys. Lett. **50,** 798–800 (1987).
18. T. Tamir, *Guided-Wave Optoelectronics,* 2nd ed., Vol. 26 of Springer Series in Electronics and Photonics (Springer-Verlag, New York, 1990).
19. Calculated with program SLAB_BETA, written by Marc Surrette of Naval Research Laboratories, Washington, D.C., 1991.
20. B. L. Anderson and P. L. Fuhr, "Twin-fiber interferometric method for measuring spatial coherence," Opt. Eng. **32,** 926–932 (1993).
21. Commercially available, for example, from New Focus, Sunnyvale, California.